

Measuring Cosmic Ray Composition at the Knee with SPASE-2 and AMANDA-II

K. G. ANDEEN[1], C. SONG[1] AND K. RAWLINS[2] FOR THE ICECUBE COLLABORATION [A].
[1] *IceCube Collaboration, University of Wisconsin-Madison, 1150 University Ave, Madison, WI*
[2] *University of Alaska Anchorage, 3211 Providence Dr, Anchorage, AK*
kandeen@icecube.wisc.edu ; [A] *See special section of these proceedings*

Abstract: Important information pertaining to the origin of high-energy cosmic rays can be gained by studying their mass composition in the region of the knee ($\sim$ 3 PeV). Thus, air showers have been observed at the South Pole using the SPASE-2 detector, which measures the electronic component at the surface, and the AMANDA-II neutrino telescope, which measures the coincident muonic component in deep ice. These two components, together with a Monte Carlo simulation and a well-understood analysis method, yield the relative cosmic ray composition in the knee region. We report on the efficacy of a new neural network technique for obtaining a composition result with the SPASE-2/AMANDA-II detectors.

Introduction

Cosmic ray composition studies can provide a greater understanding of the origin of cosmic rays, and thus lead to an increased understanding of the physical processes which accelerate these particles to Earth. At energies up to 10^{14} eV, the mass composition of cosmic rays can be measured directly; however, due to the low flux, the mass composition above 10^{14} eV must currently be gleaned from indirect measurements, involving the examination of the extensive air shower produced by the primary particle in the atmosphere. By utilizing more than one component of the air shower, such as the electronic and muonic components, an analysis technique can be developed that leads to a composition measurement.

Detectors and Reconstruction

The detectors used for this analysis the South Pole Air Shower Experiment (SPASE-2) and the Antarctic Muon And Neutrino Detector Array (AMANDA-II). The SPASE-2 detector is situated on the surface of the South Pole and is composed of 30 stations in a 30 m triangular grid. Each station contains four 0.2 m^2 scintillators. The AMANDA-II detector lies beneath the surface of the ice, located such that the center-to-center separation between AMANDA-II and SPASE-2 is about 1730 m, with an angular offset of 12°. AMANDA-II consists of 677 optical modules (OMs) deployed on 19 detector strings at depths between 1500 and 2000 m. Each OM contains a photomultiplier tube which can detect the Cherenkov light emitted by particles–namely muon bundles–passing through the ice. Besides a composition analysis, this coincident detector configuration allows for calibration as well as measurement of the angular resolution of the AMANDA-II detector [1].

For this preliminary analysis, coincident data from the years 2003-2005 are used, with a total livetime of 369 days. For comparison with the data, Monte Carlo simulated proton and iron showers with energies between 100 TeV and 100 PeV have been produced using the MOCCA air shower generator [5] and the SIBYLL v1.7 interaction model [8]. These events are then propagated through the ice, and the detector response of AMANDA-II is simulated using AMASIM. An E^{-1} spectrum is used for generation, but for analysis the events are re-weighted to the cosmic ray energy spectrum of $E^{-2.7}$ at energies below the knee at 3 PeV, and $E^{-3.0}$ above it. Both the data and Monte Carlo are then put through the same reconstruction chain.

The first step in the reconstruction is to find the incoming direction of the air shower, as well as

the core position and shower size. The direction can be computed from the arrival times of the charged particles in the SPASE-2 scintillators, while the shower core position and shower size are acquired by fitting the lateral distribution of particle density to the Nishimura-Kamata-Greisen (NKG) function and then evaluating the fit at a fixed distance from the center of the shower (in this case 30 m) [3]. This parameter, called S30, has units of particles/m^2 and will be referred to throughout this paper as a measure of the electronic part of the air shower .

The next step in the reconstruction provides a measure of the muon component of the air shower, which is carried out using the combination of the two detectors. The core position of the shower measured at SPASE-2 is kept fixed as a vertex from which θ and ϕ are varied in the ice to obtain a good fit of the track direction in AMANDA-II. The expected lateral distribution function (LDF) of the photons from the muon bundle in AMANDA-II is then computed, fit to the OM hits, and evaluated at a perpendicular distance of 50 m from the center of the shower [7]. This parameter, called K50, has units of photoelectrons/OM and will be used throughout the rest of this paper as the measure of the muon component of the air shower.

Analysis Details

Once the reconstruction has been completed, it is important to find and eliminate poorly reconstructed events. Thus, as in the previous analysis [7], events have been discarded which:

- have cores outside either the area of SPASE-2 or the volume of AMANDA-II,
- have too low an energy to be well-reconstructed in both detectors,
- have an unphysical reconstructed attenuation length of light in the ice.

After these cuts have been made, it can be seen in Figure 1 that our two main observables, S30 and K50, form a parameter space in which primary energy and primary mass separate. This is expected, as the showers associated with the heavier primaries develop earlier in the atmosphere and

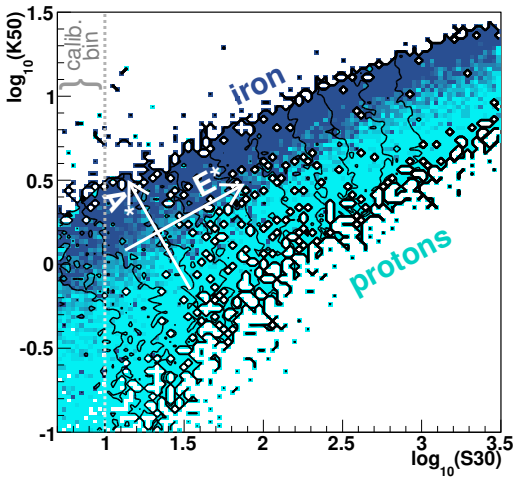


Figure 1: The two main observables, $\log_{10}$(K50) vs $\log_{10}$(S30), in the Monte Carlo simulation. The black contour lines depict gradients in energy. The axes along which mass (A*) and energy (E*) change in a roughly linear way are drawn in white, and the low-energy calibration bin is also labeled.

hence have more muons per electron by the time they reach the surface than the showers associated with lighter primaries [4]. This means that K50, which is proportional to the number of muons in the ice, will be higher for heavier primaries than for lighter primaries of the same S30, as is observed.

In the three-year data set used for this analysis, 105,216 events survive all quality cuts. It is interesting to notice that in the previous analysis, using the SPASE-2/AMANDA-B10 detector, the final number of events for one year was 5,655. Furthermore, the larger detector used here is sensitive to higher energy events. The significant increases in both statistics and sensitivity are the basis for performing a new analysis.

Calibration

To accurately measure the composition using both electron and muon information reconstructed as described above, the Monte Carlo simulations must represent the overall amplitude of light in the ice very well. However, the overall light ampli-

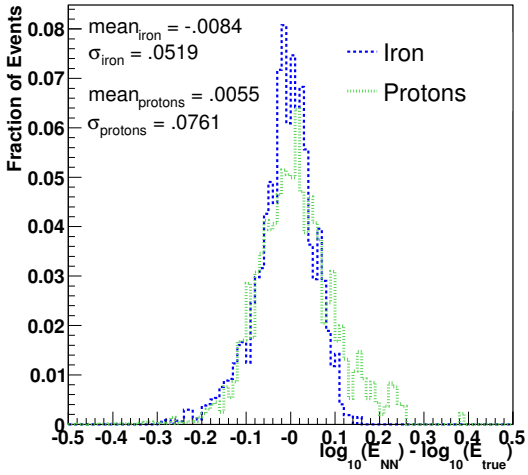


Figure 2: The energy resolution of the neural network for output energies between 1 and 10 PeV for proton and iron showers.

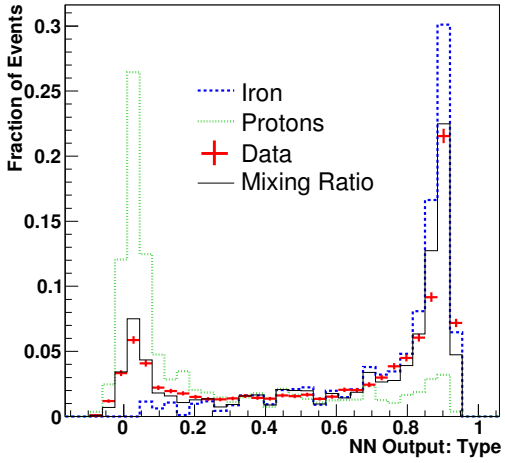


Figure 3: The neural network output for particle type with $\log_{10}(E_{NN}/GeV)$ between 6.0 and 6.2. The three-year data set is compared to the Monte Carlo generated proton and iron showers, and a mixing ratio is found which represents the data.

tude is subject to systematic errors in the simulation. Therefore, it is important to calibrate the composition measurement at low energies where direct measurements of cosmic ray composition are available from balloon experiments. A vertical "slice" of events from Figure 1, corresponding to S30 between 5 and 10 m^{-2}, is used to perform this calibration. The K50 values of the data adjusted by an offset, chosen such that the distribution of K50 best matches a 50%-50% mixture of protons and iron [2, 7]. This mixture corresponds to <lnA> = 2, which is an approximation to the value indicated by direct measurements [6].

The Neural Network

Similar past analyses [2] exploited the fact that the relationship between K50/S30 and mass/energy is approximately linear. One can then rotate to the mass/energy coordinate plane, labeled as A*/E* in Figure 1, and utilize further analysis techniques to extract the energy and mean log mass after the rotation. However, the relationship is not perfectly linear, nor should exact linearity necessarily be expected. In fact, as seen in Figure 1, the non-linear effects become more pronounced at higher energies. As the data set for this new analysis has more statistics at high energies than previous analyses, it has become important to find a technique that can resolve these events with accuracy. A neural network should be able to take these non-linear effects into account.

The neural network chosen for this analysis was the TMultiLayerPerceptron class from ROOT, which is a simple, feed-forward network, although other neural networks were also tested with similar results. The network configuration which best separates the pure proton from the pure iron scenarios and yields the best energy resolution in the Monte Carlo was a very simple 2:5:2 network, meaning there are two input variables, five hidden nodes, and two output variables. In this case, the two input variables are $\log_{10}$(K50) and $\log_{10}$(S30), and the two outputs are energy and particle type (0 for protons, 1 for iron). The network is trained on half of the Monte Carlo and tested on the other half (to evaluate its effectiveness) before being applied to the data. Figure 2 shows the energy resolution of the neural network for proton and iron showers. The "type" output of the neural network for one

energy bin is plotted in Figure 3. Notice that, since it was trained on pure proton and iron samples, the neural network tends to classify every event strictly as one or the other, resulting in the strong peaks in the data at 0 and 1. It is expected that the simulation of more primary nuclei would yield a more accurate result.

It is assumed that the data can be described by some mixture of proton and iron showers, and a technique is developed to find the mixing ratio in each energy bin which best fits the data. In order to find this proportion, the proton, iron, and data outputs are normalized and a minimization technique is applied. The result is one mixing ratio for each "slice" in energy; an example of this is shown by the solid black line in Figure 3 This method was verified using various mixtures of proton and iron simulations as input "data" and comparing with the non-mixed monte-carlo results. The ratio of heavy particles in each energy bin can also be expressed as the mean log mass. The difference between <lnA> for the neural network technique described herein and <lnA> for a rotation method similar to that used for the previous SPASE-2/AMANDA-B10 analysis is reported in Figure 4. (Note that the same data set was used for both methods.)

Discussion

It is clear from Figure 4 that the percent difference in <lnA> between the two types of analysis methods is generally quite small, especially below $\log_{10}$(E/GeV) = 6.8, which is the highest energy measured in the previous analysis. Furthermore, it seems promising that the percent difference increases at higher energies where the neural network is expected to be more reliable. The systematic errors for this data sample have yet to be fully examined, and a new Monte Carlo simulation with a variety of primary nuclei–including helium, carbon and oxygen in addition to protons and iron–is currently being generated. Nevertheless, there is a clear indication that the neural network technique is a valid method for understanding SPASE-2/AMANDA-II data, and it is hoped that, together with the new simulation and new data from the IceCube/IceTop coincident detectors, this new technique will allow us to probe energies up to 10^{18} eV.

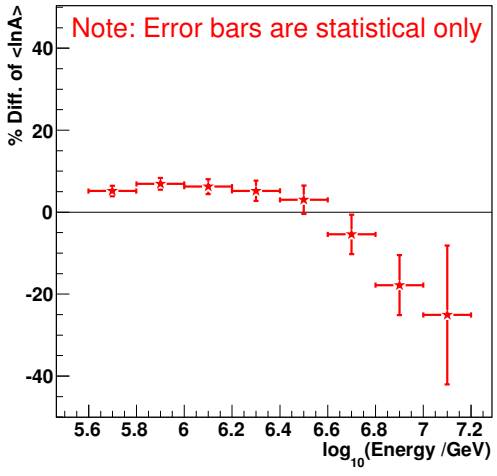


Figure 4: The percent difference in <lnA> between two analysis techniques applied to the same three-years of SPASE-2/AMANDA-II data.

Acknowledgements

The authors would like to acknowledge support from the Office of Polar Programs of the United States National Science Foundation.

References

[1] J. Ahrens et al. *Nuclear Instruments and Methods*, 522:347–359, 2004.

[2] J. Ahrens et al. *Astroparticle Physics*, 21:565–581, 2004.

[3] J.E. Dickinson et al. *Nuclear Instruments and Methods*, 440:95–113, 2000.

[4] T. Gaisser. *Cosmic Rays and Particle Physics*. Cambridge University Press, 1988.

[5] A.M. Hillas. *Proceedings of the 24th International Cosmic Ray Confrence*, 1:270, 1995.

[6] J.R. Hörandel. *International Journal of Modern Physics A*, 20(29):6753–6764, 2005.

[7] K. Rawlins. PhD thesis, University of Wisconsin, Madison, 2001.

[8] R.S. Fletcher T.K. Gaisser, P. Lipari and T. Stanev. *Phys. Rev. D*, 50:5710, 1994.